Reduce the stretch in surface flattening by finding cutting paths to the surface boundary

Charlie C. L. Wang* **Yu Wang** **Kai Tang** **Matthew M. F. Yuen**

Department of Mechanical Engineering, Hong Kong University of Science and Technology,

Clear Water Bay, Kowloon, Hong Kong

Abstract

This paper presents a method for finding cutting paths on a 3D triangular mesh surface to reduce the stretch in the flattened surface. The cutting paths link the surface boundary and the nodes where the Gaussian curvature is high, and their total length is minimized. First, a linear algorithm for computing an approximate boundary geodesic distance map is introduced; the map encapsulates the undirected geodesic distance from every triangular node to the surface boundary approximately. This is followed by determining the undirected shortest paths passing through all the nodes where the Gaussian curvature is larger than a threshold. The cutting paths walk along the triangular edges of the given surface. Compared with other similar approaches, our method reaches a faster speed, and can deal with surfaces with widely distributed curvatures.

Keywords: surface flattening, Gaussian curvature, cutting path, shortest path, and geodesic distance.

1. Introduction

Surface flattening plays a prominent role in engineering and manufacturing applications, such as aircraft design, vehicle design, garment design, etc. Isometric surface development is also a key procedure for texture mapping in computer graphics. It is known that flattening a 3D surface into a plane introduces surface metric (angle, distance, areas) stretch unless the surface has zero Gaussian curvature everywhere [1] - Gaussian curvature is the product of the maximum and minimum normal curvatures at a given point. Thus, the stretch depends directly on the Gaussian curvature of the given surface. Cutting the surface across points of high Gaussian curvature will reduce the stretch in the flattened surface. However, since cutting paths modify and elongate the boundary of a surface, they often introduce additional constraints to the following applications (e.g., they may lead to discontinuity in texture mapping). Therefore, the length of cutting paths has to be minimized. Subdividing triangles might lead to difficulties in the following applications after surface flattening

* Corresponding Author: wangcl@ust.hk

(e.g., some finite element applications), so our cutting paths walk along the triangular edges of the given triangular mesh surface.

When introducing our algorithm, the following definitions are necessary.

Definition 1.1 The *boundary geodesic distance map* is a map that encapsulates the undirected geodesic distance from every node to the boundary on the given mesh surface.

Definition 1.2 A *flipped triangle* is a triangle whose normal direction after flattening is along the negative z-axis while the normal direction of other flattened triangles is along the positive z-axis.

Contribution: This paper describes a method to find the cutting paths on a 3D triangular mesh surface to reduce the stretch in the flattened surface. The shortest cutting paths connecting all nodes where Gaussian curvature is larger than a threshold are generated according to our newly defined boundary geodesic distance map. The map encapsulates the undirected geodesic distance from every triangular node to the surface boundary approximately, and can be computed in linear time. The cutting paths on surfaces with widely distributed curvatures can also be found by generating cuts during the flattening process. Compared with other similar approaches, our method reaches a faster speed while generating an acceptable result; it can deal with surfaces with widely distributed curvatures.

After reviewing the related work in section 2, the rest of the paper is organized as follows. In section 3, a linear algorithm is introduced to compute the approximate boundary geodesic distance map of a surface; this is followed by generating the approximate shortest path from a selected node to the surface boundary by the map. In section 4, we propose a reduction of the stretch in the flattened surface by adding shortest cutting paths from high Gaussian curvature nodes to the surface boundary. During the surface flattening process, cutting paths are also incorporated to prevent flipped triangles. Finally, in section 5, experimental results are shown and discussed.

2. Related Work

Carmo (1976) [1] defined a developable surface as: for a ruled surface – $X(t,v)=\alpha(t)+v\beta(t)$, it is developable if β, $\frac{d\beta}{dt}$ and $\frac{d\alpha}{dt}$ are coplanar for all points on X (where $\alpha(t)$ is the *base curve* and $\beta(t)$ is the *director curve* of $X(t,v)$). The simplest examples of developable surfaces are cylinders and cones, and a simple and representative example of non-developable surfaces is sphere. Every surface enveloped by a one-parameter

family of planes is a developable surface. Generally, a surface is developable if and only if the Gaussian curvature of every point on it is zero. It is difficult to satisfy this condition when given a freeform polygonal mesh surface. Thus, it is important to introduce cutting paths to make the given surface as close as possible to the developable condition.

Gaussian curvature is the product of the maximum and minimum normal curvatures at a given point [1]. However, since differential geometry analyzes surfaces that are sufficiently differentiable, the equation for calculating the Gaussian curvature cannot be applied to a mesh surface directly. A discrete Gaussian curvature computing method is needed. Kobbelt et al. [2] gave the formulas of discrete Gaussian curvature based on the fact that meshes can be interpreted as approximations of smooth surfaces. The idea of their approach is to discretize a theorem for defining the Gaussian curvature on a smooth surface derived from a theorem by Rodrigues [1]. In the same way, Sheffer [3] gave another Gaussian curvature approximation, which is scale independent. In our approach, we adopt the formula of Kobbelt et al. [2] to compute the Gaussian curvature of every internal triangular node on a mesh surface.

Insertion of cuts or darts in surface flattening has been studied for a long time. Parida and Mudur (1993) [4] presented an algorithm to obtain planar development (within acceptable tolerances) of complex surfaces with cuts and overlaps only in specified orientations. Their algorithm first obtains an approximate planar surface by flattening triangles, cracks are generated while triangles are flattened one by one; and then, they reorient cracks and overlap parts in the developed plane to satisfy orientation constraints. Their algorithm might generate many cracks and calculation errors. Aono et al. [5, 6] introduced a reverse approach to surface flattening, which inserts darts to fit a woven cloth model to a curved surface. Other approaches are based on local strain energy minimization technology [7, 8]. The approach of Wang et al. [9] generates the cutting line from the stretch energy distribution map; however, the length of cutting paths is not considered in their paper. Recently, Sheffer [3] tried to find the shortest cutting path that passes through the nodes with high Gaussian curvature to reduce the parameterization distortion of the triangulated surface. Unfortunately, this method is not able to find protrusions with widely distributed curvatures (e.g., looped cylindrical surfaces); and a modified Dijkstra algorithm is applied in this method to compute the shortest paths, whose running time is $O(E \log N)$, where N is the number of triangular nodes and E is the number of triangular edges. Our method presented in this paper can compute the shortest path from a node to the surface boundary in linear time; and the cutting paths on the surface with widely distributed curvatures are generated while preventing flipped triangles in surface flattening.

The single source shortest path problem (SSSP) is one of the classic problems in algorithmic graph theory [10]: given a weighted graph with a source vertex, find the shortest path from the source vertex to all other vertices in the graph. For the shortest path problem on a polygonal surface, approaches based on Dijkstra algorithm [11] are most popular solutions [3, 12, 13]. Their computing time is non-linear though. Thorup (1997) [14] presented a method to compute the undirected single source shortest paths in linear time; this is the fastest solution. Here, our problem is different from SSSP. We need to select a node from candidate nodes where Gaussian curvature is larger than a threshold. The final selected node should have the shortest geodesic distance to the surface boundary among the candidate nodes. The algorithm of Thorup cannot be directly applied here since it cannot give the geodesic distance from multiple points to the surface boundary in linear time. Thus, the newly defined boundary geodesic distance map is needed, which is different from the weighted graph with a source vertex in SSSP. After the node is selected, the shortest cutting path from it to the surface boundary walking along the triangular edges can also be computed in linear time.

3. Approximate Shortest Path to Surface Boundary

In this section, we introduce a method to approximate the shortest path from a selected node to the surface boundary in linear time. First, a boundary geodesic distance map, which indicates the undirected geodesic distance from every triangular node to the boundary on the mesh surface, is computed in linear time. After that, the approximate shortest path is generated from the map, also in linear computing time.

3.1 Boundary geodesic distance map

We generate the boundary geodesic distance map using a boundary advancing method, which progressively moves the event list L_v of the triangular nodes from the boundary to the center of the surface. During the movement, the geodesic distance between the event list before and after moving is used to update the boundary geodesic distance of every passed node. The given triangular mesh M is stored in a graph $G(v,e)$. $G(v,e)$ is composed of the vertices and the edges of M. Every node has its adjacent nodes and edges stored; and every edge has its bounding nodes stored. The geodesic distance from every vertex v_i to the surface boundary is stored as a weight factor W_{v_i}. Before moving the event list, the W_{v_i} of every internal vertex is initialized as $+\infty$; the W_{v_i} of every boundary vertex is set to zero; and the length of every edge e_j is calculated and stored. Our algorithm repeatedly moves L_v from the boundary to the center of M; during the movement, the W_{v_i} of

the nodes adjacent to L_v are updated. The pseudo-code for the boundary geodesic distance map generation is given as follows.

Algorithm MapGeneration(G)
Input: A graph $G(v,e)$ of the given mesh surface M.
Output: The updated weight factor W_{v_i} of every triangular node.

1. **for** every node $v_i \in G$ {
2. $W_{v_i} \leftarrow +\infty$;
3. Set the passed flag of v_i – fp_{v_i} to **false**;
4. **if** (v_i on the boundary)
5. Add v_i to L_v, $W_{v_i} \leftarrow 0$, and set the passed flag of v_i – fp_{v_i} to **true**;
6. }
7. Calculate the length l_{e_j} of every edge $e_j \in G$;
8. $L_v' \leftarrow \phi$;
9. **do**{
10. **for** every node $v_k \in L_v$ {
11. **for** every node v_j adjacent to v_k {
12. **if** ((W_{v_k} + the length of edge $v_j v_k$) < W_{v_j}), **then** $W_{v_j} \leftarrow W_{v_k}$ + the length of edge $v_j v_k$;
13. **if** (fp_{v_j} is **false**), **then** add v_j to L_v' and set fp_{v_j} to be **true**;
14. }
15. }
16. Replace L_v by L_v' and empty L_v';
17. }**while**($L_v \neq \phi$);

After running *MapGeneration(G)*, the weight factor W_{v_i} of every node indicates the approximate geodesic distance from the node v_i to the boundary of M. The complex of W_{v_i}, called W, and the graph $G(v,e)$ comprise the approximate boundary geodesic distance map $\mathrm{B} = W + G$. The visualization for the isohypses generated from B to the surface given in Fig. 1a is shown in Fig. 1c. From Fig. 1c, we find that our boundary geodesic distance map approximately indicates the geodesic distance from every surface point to the boundary.

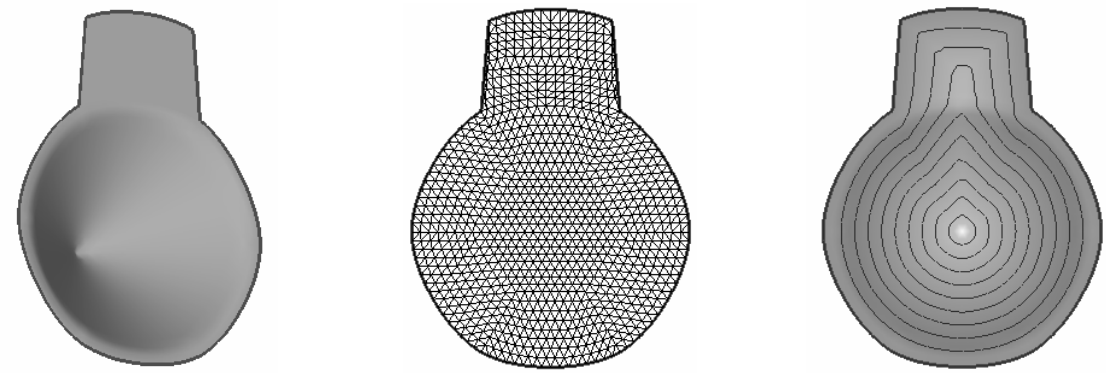

(a) given surface **(b) mesh representation** **(c) isohypse of** B

Fig. 1 Boundary geodesic distance map

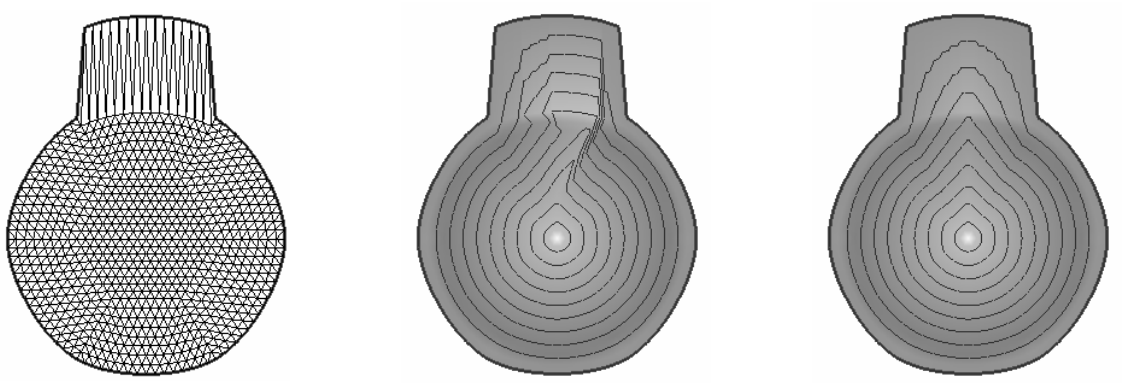

(a) surface with non-uniform edge lengths **(b) result generated by** MapGeneration(G) **(c) result generated by** AdaptiveMapGeneration(G)

Fig. 2 Approximation error generated by non-uniform edge lengths

In ***Algorithm*** MapGeneration(G), we assume that the lengths of edges are close to each other; so the weight difference between the nodes of L_v and L_v' is a constant. However, when the edges in M do not have the same length, an approximation error will be generated by ***Algorithm*** MapGeneration(G) since the weight difference between the nodes of L_v and L_v' is no longer a constant. For example, in the surface shown in Fig. 2a which has the same 3D shape as the one in Fig. 1a, the lengths of some edges are much longer than others; the isohypses of B generated by ***Algorithm*** MapGeneration(G) are shown in Fig. 2b, which are apparently distorted. To reduce this error, when selecting a node to add to L_v', the weight difference between the nodes of L_v and L_v' should be controlled. Only nodes that make the weight difference less than some threshold value will be added into L_v'. We use the length of the shortest triangular edge as the incremental step of the threshold in our modified algorithm. Also, the node in L_v should also be added to L_v' if the event list has not passed any of its adjacent nodes before. The modified algorithm is adaptive with the length of triangular edges. It is outlined below as ***Algorithm*** AdaptiveMapGeneration (G).

Algorithm AdaptiveMapGeneration(G)
Input: A graph $G(v,e)$ of the given mesh surface M.
Output: The updated weight number W_{v_i} of every triangular node.

1. **for** every node $v_i \in G$ {
2. $W_{v_i} \leftarrow +\infty$;
3. Set the passed flag of $v_i - fp_{v_i}$ to **false**;
4. **if** (v_i on the boundary)
5. Add v_i to L_v, $W_{v_i} \leftarrow 0$, and set the passed flag of $v_i - fp_{v_i}$ to **true**;
6. }
7. Calculate the length l_{e_j} of every edge $e_j \in G$, and store the minimum edge length as $l_{\min}$;
8. $L_v' \leftarrow \phi$;

9. $\lambda \leftarrow l_{\min}$;
10. **do**{
11. **for** every node $v_k \in L_v$ {
12. **for** every node v_j adjacent to v_k {
13. **if** ((W_{v_k} + the length of edge $v_j v_k$) < W_{v_j}), **then** $W_{v_j} \leftarrow W_{v_k}$ + the length of edge $v_j v_k$;
14. **if** ((fp_{v_j} is **false**) and ($W_{v_j} < \lambda$)), **then** add v_j to L_v' and set fp_{v_j} to **true**;
15. }
16. }
17. **for** every node $v_k \in L_v$
18. **if** any fp_{v_i} of its adjacent node v_j is **false**, **then** add v_k to L_v';
19. Replace L_v by L_v' and make L_v' empty;
20. $\lambda \leftarrow \lambda + l_{\min}$;
21. }**while**($L_v = \phi$);

After applying ***Algorithm*** AdaptiveMapGeneration (G) to the mesh surface given in Fig. 2a, the isohypses of the result are shown in Fig. 2c. Fig. 3a shows the weight factor of nodes in Fig. 2b; Fig. 3b shows the weight factor of nodes in Fig. 2c; and Fig. 3c shows the weight factor of nodes in Fig. 1c. Comparing them, it is easy to find that the lengths of triangular edges have less influence on the result of ***Algorithm*** AdaptiveMapGeneration (G). Thus, the isohypses in Fig. 1c and 2c are the same except in the area where there is no any triangular node.

Computing time analysis: For ***Algorithm*** MapGeneration(G), the running time of step 1-6 is $O(N)$, where N is the number of triangular nodes; the running time of step 7 is $O(E)$, where E is the number of triangular edges; and during step 9-17, since every node visits its adjacent nodes once – in other words, every edge is passed twice, the running time is $O(E)$. Therefore, the running time of ***Algorithm*** MapGeneration(G) is $O(N+E)$. For ***Algorithm*** AdaptiveMapGeneration(G), the running time of step 1-6 is also $O(N)$; and the running time of step 7 is $O(E)$. For the running time of step 11-16, every node visits its adjacent nodes $INT(\|v_j v_k\| / l_{\min})$ times, where $INT(\ldots)$ denotes the function to round a number down to the nearest integer. Thus, the running time in the worst case is $O(TE)$, where $T = INT(l_{\max} / l_{\min})$, and $l_{\max}$ and $l_{\min}$ denote the maximum and minimum edge length on the given surface M. The running time of step 17-18 is $O(E)$ since every node visits its adjacent nodes once. In summary, the running time of ***Algorithm*** AdaptiveMapGeneration(G) is $O(N+(T+1)E)$. Generally, T is a small number (e.g., from 1 to 100). Therefore, the running time of the ***Algorithm*** AdaptiveMapGeneration(G) is also linear in N and E.

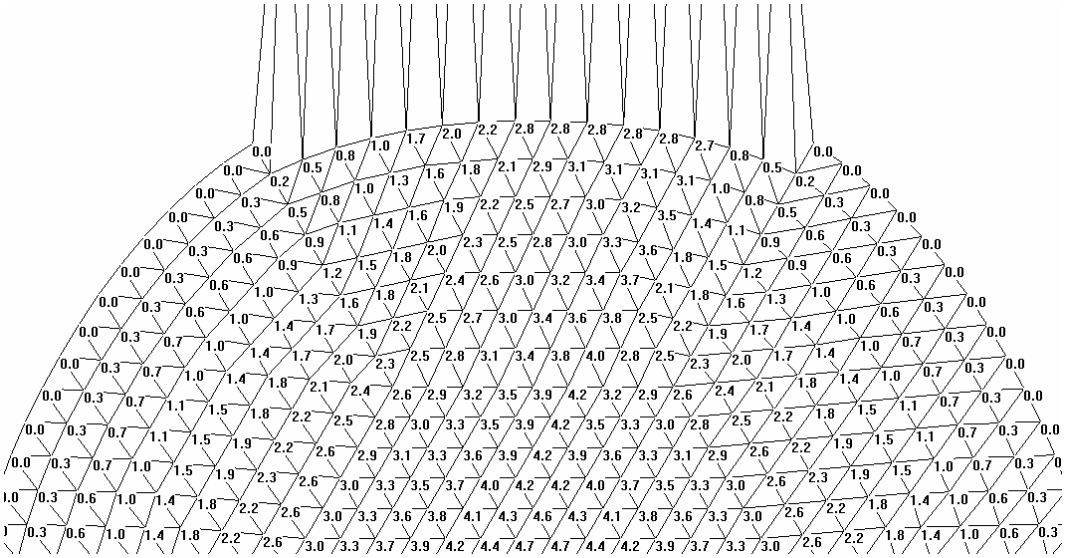

(a) weight factor of nodes in Fig. 2b

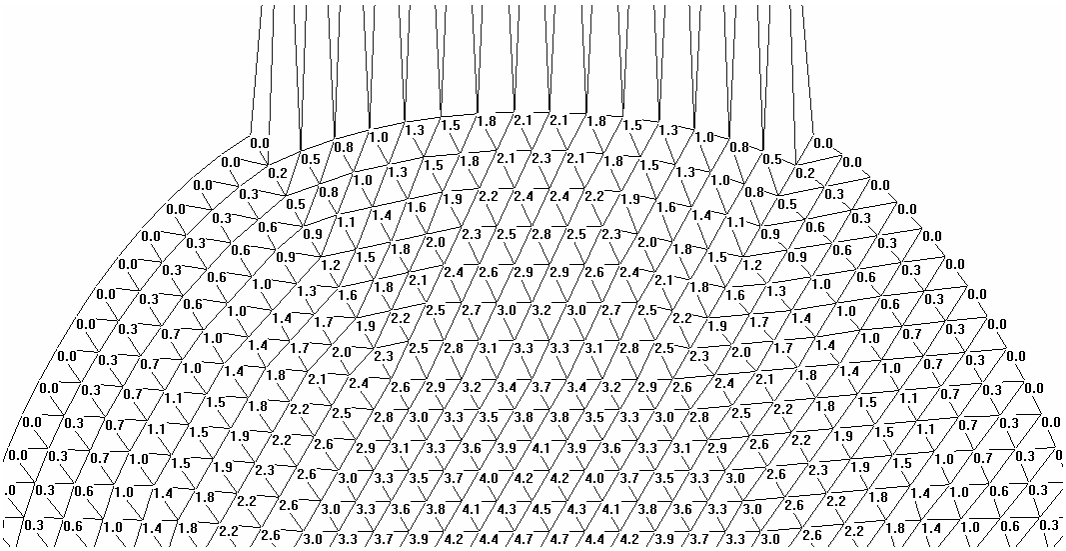

(b) weight factor of nodes in Fig. 2c

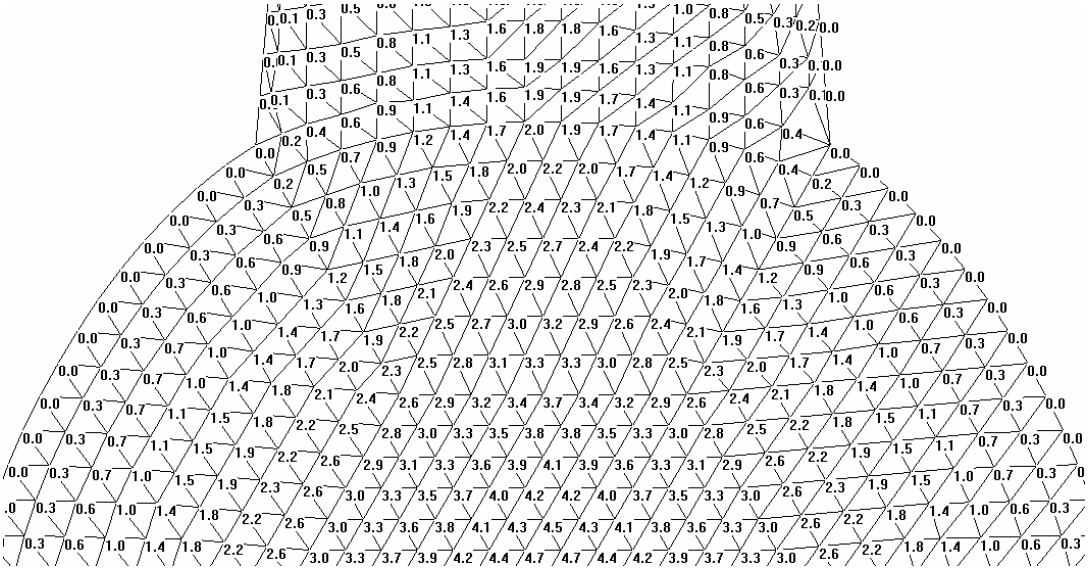

(c) weight factor of nodes in Fig. 1c

Fig. 3 Boundary geodesic distance map by weight factors

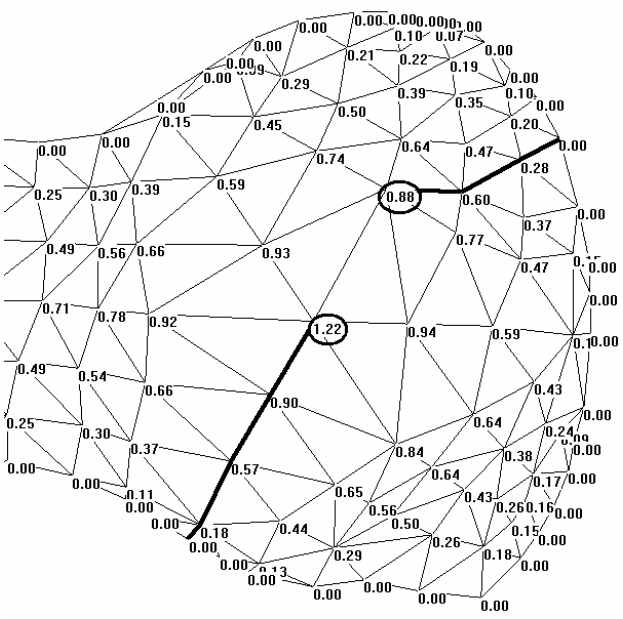

Fig. 4 Path generated from the boundary geodesic distance map

3.2 Generate approximate shortest path

We generate the approximate shortest path from a select node v_s to the surface boundary by the steepest descent method [15] according to the boundary geodesic distance map. For any selected triangular node $v_i \in G$, all its adjacent nodes are candidates for forming the path. We choose the node v_j, whose descent function $f_d(v_i, v_j)$ has the maximum value among all the adjacent nodes of v_i. The definition of $f_d(v_i, v_j)$ is

$$f_d(v_i, v_j) = (w_{v_i} - w_{v_j}) \Big/ \left\| v_i v_j \right\| . \tag{1}$$

Starting from node v_s, after searching for the adjacent nodes with the maximum $f_d(v_i, v_j)$ one by one, the final path is generated. For example, in Fig. 4, the circled node is v_s, and the bolded edges are the final path. The pseudo-codes of the path generation algorithm are given below as ***Algorithm*** PathGeneration (v_s, B).

Algorithm PathGeneration (v_s, B)
Input: Boundary geodesic distance map B of the given mesh surface M.
Output: The cutting path P, consisting of triangular edges.

1. P $\leftarrow \phi$;
2. **while**($W_{v_s} \neq 0$){
3. $v_{\max} \leftarrow$ any node adjacent to v_s;
4. **for** every node v_j adjacent to v_s
5. **if** ($f_d(v_s, v_j) > f_d(v_s, v_{\max})$), **then** $v_{\max} \leftarrow v_j$;
6. Add the edge $v_s v_{\max}$ into P;
7. $v_s \leftarrow v_{\max}$;
8. }
9. **return** P;

In the worst case, every node on the given mesh surface M visits its adjacent node once; so the computing time is $\mathrm{O}(E)$. In summary, we can generate the approximate shortest path from a selected node to the surface boundary in linear time.

4. Reduce Stretch in Surface Flattening

Using the technique of approximating the shortest path to the boundary, we develop a method to determine the cutting paths passing through all the nodes where the Gaussian curvature is higher than some given value. After that, cutting paths may also be incorporated in surface flattening to prevent flipped triangles.

4.1 Node selection

As alluded earlier, the stretch in the flattened surface depends directly on the Gaussian curvature of the given surface. Cutting the surface across points with a high Gaussian curvature can thus reduce the stretch in surface flattening. Gaussian curvature is not well defined mathematically on a polygonal mesh surface, so a discrete approximation is needed. Here, we conduct the approximation of Kobbelt et al. [2] on every internal triangular node v_i. The formula of [2] is

$$\kappa_{v_i} = \frac{2\pi - \sum_j \theta_j}{\frac{1}{3}\sum_j A_j}, \tag{2}$$

where θ_j are the inner angles adjacent to v_i and A_j are the corresponding triangle areas.

The Gaussian curvature κ_{v_i} of the nodes on the boundary of the given surface is zero since its adjacent triangles are not closed. All the triangular nodes, whose $\kappa_{v_i} > \varepsilon$, are candidates. In different cases, a different ε can be chosen. A larger ε leads to shorter cutting paths, and a smaller ε always leads to longer cutting paths. In our testing examples, we usually choose $\varepsilon = 0.8\kappa_{\max}$, where $\kappa_{\max}$ is the maximum Gaussian curvature among all the interior nodes on the given mesh surface.

4.2 Add cutting path

After the nodes whose Gaussian curvatures are higher than ε are determined and stored in a candidate notes list L_c, the shortest path connecting these nodes and the surface boundary is determined by an incremental method. First, we compute the boundary geodesic distance map B of the surface; secondly, we remove a node v_c from L_c whose weight factor w_{v_c} is a minimum in L_c; thirdly, we use ***Algorithm*** PathGeneration (v_c , B) to generate a cutting path from v_c to the surface boundary. After that, we add the newly generated path into the

surface boundary, and go back to the first step to compute the new boundary geodesic distance map. We determine the cutting path through all the candidate nodes by repeating the above steps until the candidate notes list L_c becomes empty.

In order to construct a fast algorithm, we store the candidate nodes list in a minimum heap H_c; so the computing time of any operation on a single node in H_c is $\mathrm{O}(\log N_c)$, where N_c is the number of nodes in H_c. After computing the boundary geodesic distance map of the given surface in linear time, it only takes a time of $\mathrm{O}(N_c \log N_c)$ to update the minimum heap H_c and a time of $\mathrm{O}(\log N_c)$ to remove any node v_c from H_c. Therefore, the total computing time of our algorithm is $\mathrm{O}((N+(T+1)E)N_c \log N_c)$. The pseudo-codes of our algorithm are shown as ***Algorithm*** DetermineCuttingPathReducingStretch (M). Two examples of cutting path generation are shown in Fig. 5 and 6, where the bolded curves are the determined cutting paths.

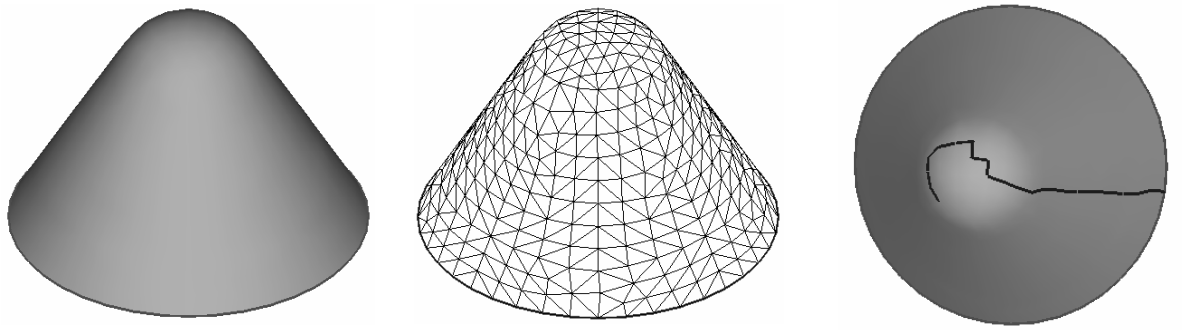

(a) given surface **(b) mesh presentation** **(c) with cutting path generated**

Fig. 5 Example I – umbrella surface

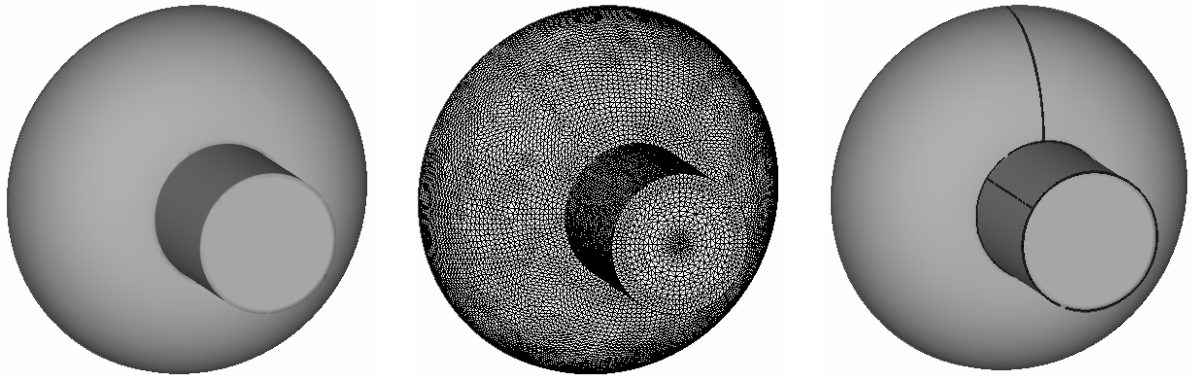

(a) given surface **(b) mesh presentation** **(c) with cutting path generated**

Fig. 6 Example II – bottle surface

Algorithm DetermineCuttingPathReducingStretch (M)
Input: The given mesh surface M with boundary B_{M}.
Output: The cutting path P* connecting B_{M} and nodes with high Gaussian curvature.

1. P* $\leftarrow \phi$;
2. **Call** AdaptiveMapGeneration (G) to generate the boundary geodesic distance map B of M;

3. **for** every internal nodes $v_i \in \mathrm{M}$
4. Compute the Gaussian curvature κ_{v_i} of v_i by eq.(2);
5. **for** every boundary node $v_b \in B_{\mathrm{M}}$
6. $\kappa_{v_b} \leftarrow 0$;
7. **for** every node $v_i \in \mathrm{M}$
8. **if** ($\kappa_{v_i} > \varepsilon$), **then** add v_i into the minimum heap H_c by the value of w_{v_i};
9. **while**($H_c \neq \phi$){
10. Remove the top node v_c from H_c;
11. **Call** PathGeneration (v_c , B) to generate the cutting path P;
12. Add P into P*;
13. Add every triangular edge in P into B_{M};
14. **Call** AdaptiveMapGeneration (G) to generate the updated B by the updated boundary B_{M};
15. Update H_c by the new w_{v_i} of every node $v_i \in H_c$;
16. }
17. **return** P*;

4.3 Surface flattening

After the surface cutting path is determined, a spring-mass model based on the energy function is used to flatten the 3D mesh surface into its corresponding 2D pattern [9]. This procedure consists of triangles flattening and planar mesh deformation. During the triangles flattening phase, triangles are flattened one by one; and a partial spring-mass system containing flattened triangles is deformed to release the strain energy during the flattening. After all the triangles are flattened, the spring-mass system will have all the triangles of the given surface. The planar triangular mesh deformation process is directed by the energy function of the spring-mass system. One example of a spring-mass system is shown in Fig. 7. In this example, nodes P_i are masses that correspond to the vertex $v_i \in \mathrm{M}$; and the links between masses P_i and P_j are springs. During deformation, if the distance between P_i and P_j on the planar surface is larger than the distance between them on the original spatial surface, we apply an attraction force between them (e.g., the force between P_0 and P_1); otherwise there will be a repellent force between them (e.g., P_0 and P_3).

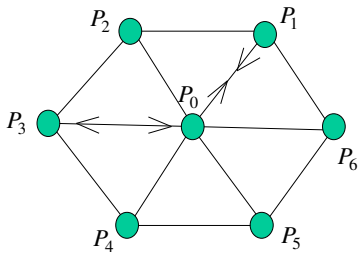

Fig. 7 Example of a node in a spring-mass system

The energy function on one single mass P_i to be minimized is

$$E(P_i) = \sum_{j=1}^{n} \frac{1}{2} C\left(\left|P_i P_j\right| - d_j\right)^2 \tag{3}$$

where C is the spring constant, $\left|P_i P_j\right|$ is the current distance between P_i and P_j on the planar surface, and d_j is the geodesic distance between v_i and v_j on the given mesh surface M. The energy function for the whole surface patch is

$$E(\mathrm{M}) = \sum_{i=1}^{N} E(P_i) . \tag{4}$$

By releasing the energy function, we can obtain the 2D pattern corresponding to the given 3D mesh surface. The surface flattening results of example I (Fig. 5) and II (Fig. 6) are shown in Fig. 8.

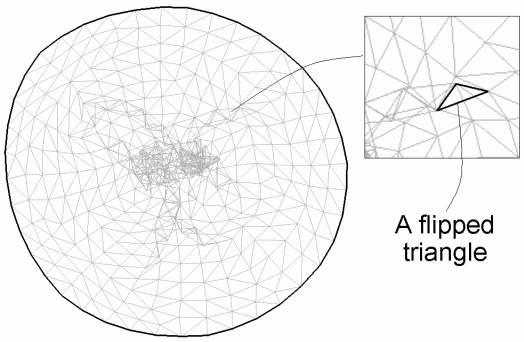

(a) result of example I without cutting paths

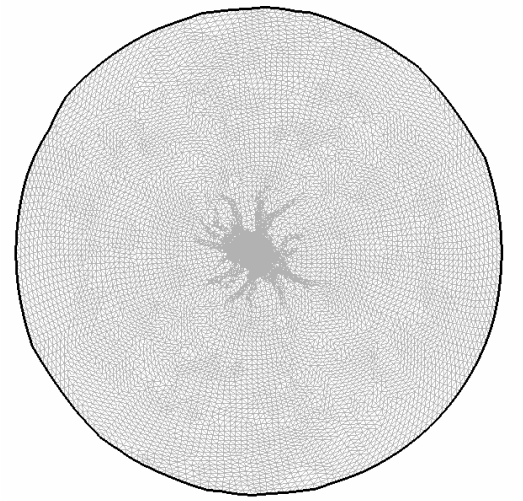

(b) result of example II without cutting paths

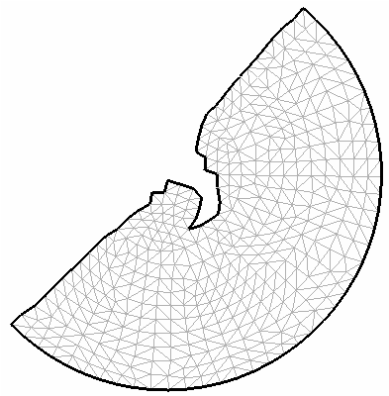

(c) result of example I with cutting paths

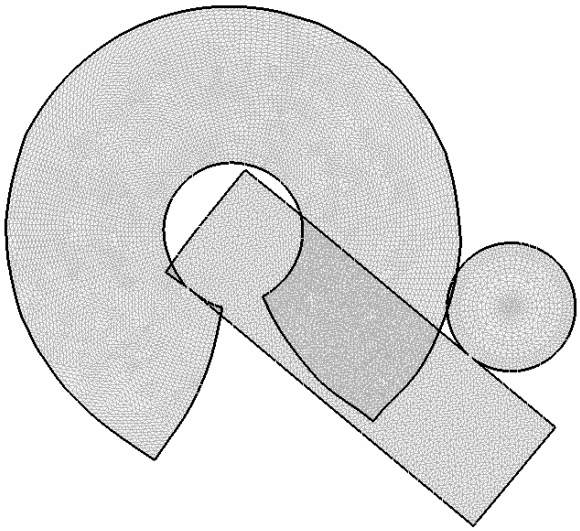

(d) result of example II with cutting paths

Fig. 8 Surface flattening results without vs. with cutting paths

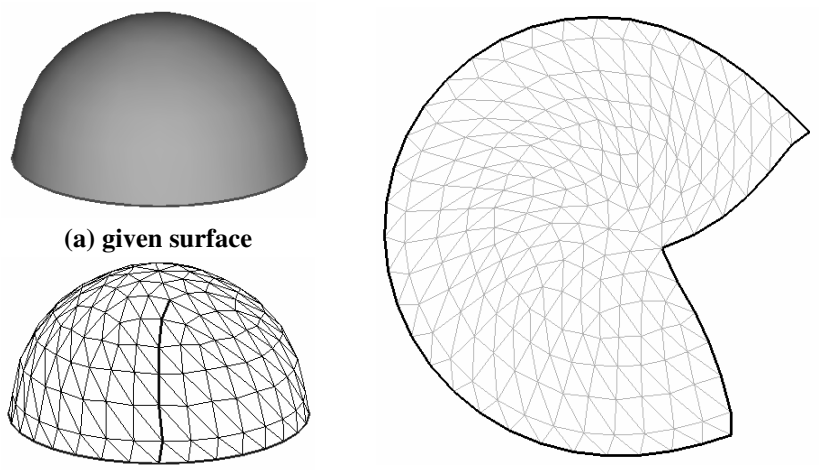

(a) given surface

(b) with cutting path

(c) surface flattening result

Fig. 9 Example III – hemisphere

4.4 More cuts generation

The ***Algorithm*** DetermineCuttingPathReducingStretch (M) cannot give efficient cutting paths to the surfaces with widely distributed curvatures (e.g., a cylindrical surface or a hemisphere). Alternative methods are introduced in this section to reduce stretch in these cases.

For the case of a surface patch with widely distributed curvatures, if the surface has only one boundary loop, we incorporate the cutting path from the flipped triangles to the surface boundary. The procedure consists of 4 steps: step 1, flatten the given mesh M by the method given in section 4.3; step 2, check the orientation of every triangle and find the flipped triangles; step 3, find the node v_m with the minimum weight factor w_{v_m} in the flipped triangles; step 4, incorporate the cutting path by calling ***Algorithm*** PathGeneration (v_m , B); then go back to step 1 until no flipped triangle is found. The cutting path determined by this method on a hemisphere and its flattening result is shown in Fig. 9.

If a surface patch with widely distributed curvatures has multiple boundary loops, we incorporate the cutting path to connect these loops. We can determine the shortest path connecting the two loops – B_1 and B_2 from a modified geodesic distance map B'. To determine B', when using ***Algorithm*** AdaptiveMapGeneration (G) to compute the geodesic distance map, in step 3-4, only the vertices on B_1 are set to be of zero weight and are passed. After determining B', the vertex v_c on B_2 with the minimum weight factor can be found. Calling this ***Algorithm*** PathGeneration (v_c , B'), we obtain the shortest path connecting the two boundary loops. The cutting path determined by this method on a cylindrical surface and its corresponding flattening result are shown in Fig. 10.

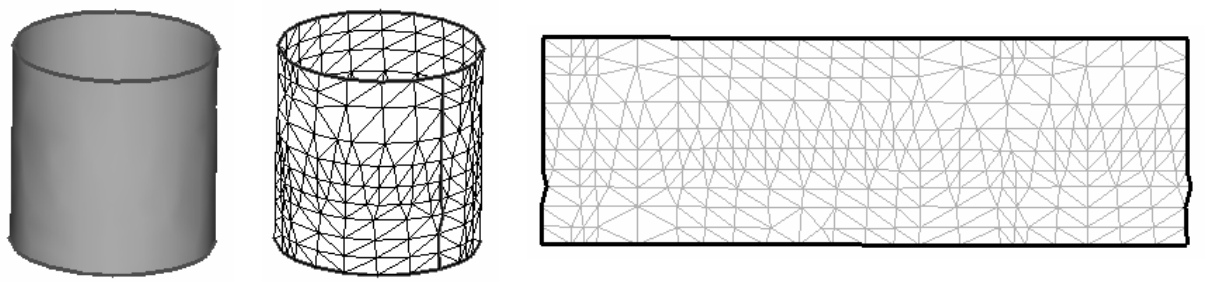

(a) given surface **(b) with cutting path** **(c) surface flattening result**

Fig. 10 Example IV – cylindrical surface

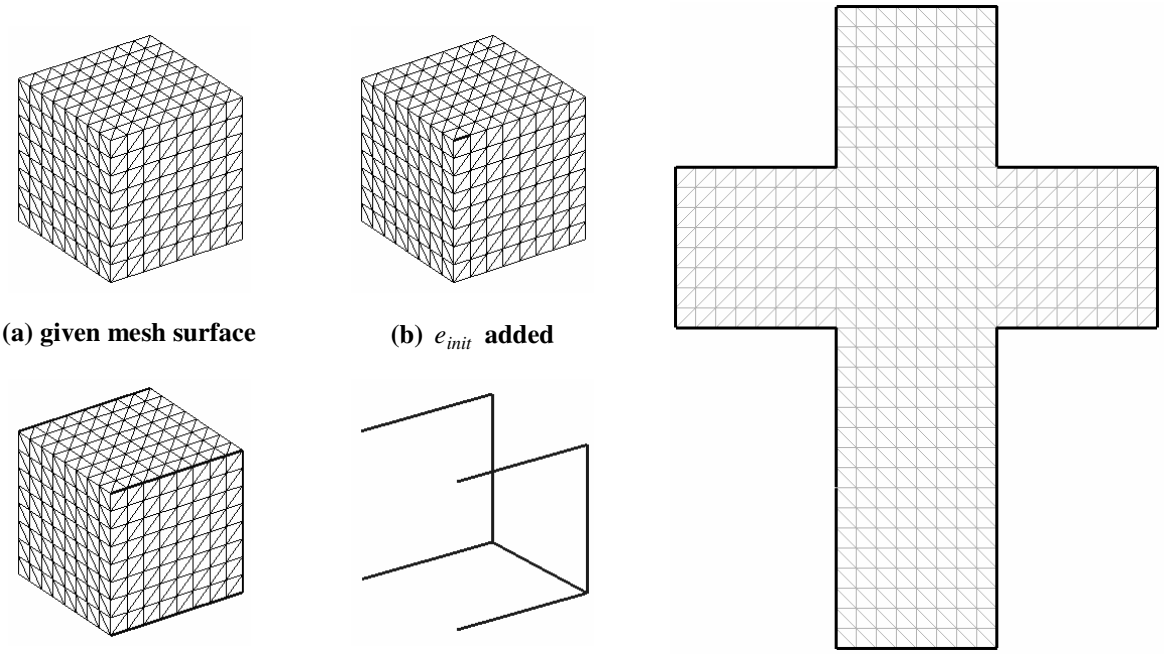

(a) given mesh surface **(b) e_{init} added**

(c) cutting path **(d) cutting path profile** **(e) surface flattening result**

Fig. 11 Example V – closed surface

When a given mesh surface M is closed, ***Algorithm*** DetermineCuttingPathReducingStretch(M) will fail, as there is no boundary to work on. With reference to [16], we only need to add an initial cutting edge e_{init} passing through the vertex $v_{\max}$, which has the maximum Gaussian curvature on M. e_{init} is the shortest adjacent triangular edge of $v_{\max}$. After e_{init} is given, we determine the final cutting path by calling ***Algorithm*** DetermineCuttingPathReducingStretch(M). A closed surface example, a cube, is shown in Fig. 11.

(a) given mesh surface

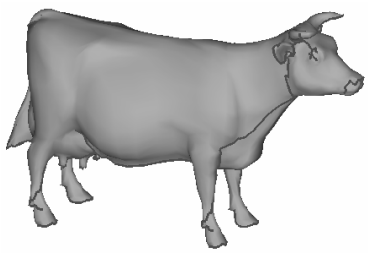

(b) with cutting lines

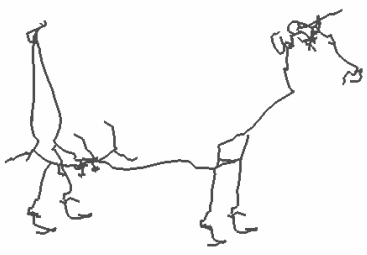

(c) profile of cutting lines in (b)

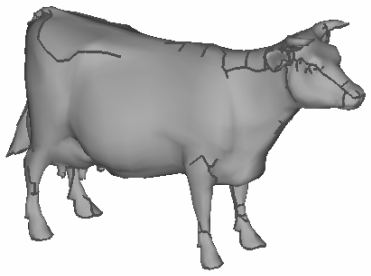

(d) more cutting lines

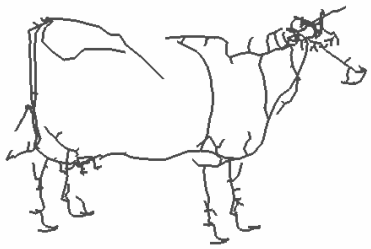

(e) profile of cutting lines in (d)

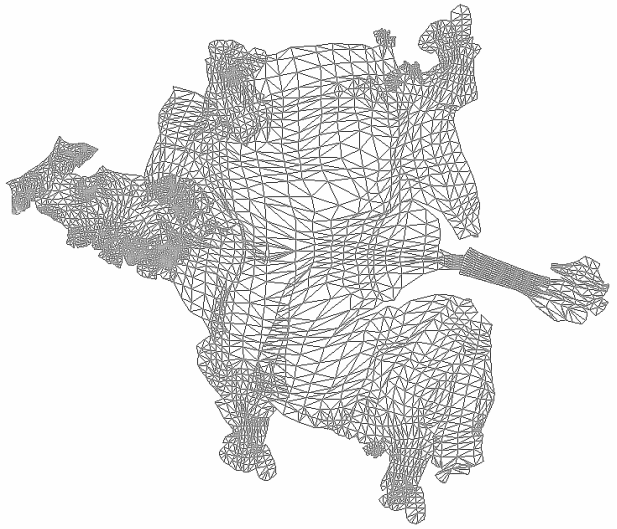

(f) surface flattening result

Fig. 12 Example VI – cow

5. Experimental Results

In general, we can determine the cutting path to reduce the stretch in surface flattening by passing through the nodes with high Gaussian curvatures. In example I, the given mesh surface has 774 triangles; when we choose $\varepsilon = 0.8\kappa_{\max}$ as the threshold, 23 cutting edges passing through 7 high curvature nodes are computed in less than one second. In example II, the given mesh surface has 21122 triangles; when we choose $\varepsilon = 0.8\kappa_{\max}$ as the threshold, 268 cutting edges passing through 200 high curvature nodes are determined in 93 seconds.

In order to compare our method with the others that are based on the similar idea of using cutting paths, we select a same example as [3] – the cow (shown in Fig. 12a), which has 5804 triangles. When we choose $\varepsilon = 0.8\kappa_{\max}$ as the threshold, 478 cutting edges passing through 279 high curvature nodes (shown in Fig. 12b and 12c) are computed in 47 seconds. This compares favorably to the computing time reported in [3] which is close to two minutes when 326 cutting edges passing through 98 nodes are incorporated. Since the cow is a surface with widely distributed curvatures, more cutting edges should be introduced to reduce the stretch by the method of section 4.4. Fig. 12d and 12e show the final cutting edges, and Fig. 12f shows its corresponding surface flattening result. All tests in this paper were conducted on a PIII 600 MHz PC with 128MB RAM.

6. Conclusion

In this paper, we develop a method for finding the cutting paths on a 3D triangular mesh surface to reduce the stretch on the flattened surface. The length of cutting paths is minimized. First, a linear algorithm to compute an approximate boundary geodesic distance map is developed. The algorithm is adaptive to different lengths of triangular edges. After that, the undirected shortest path from a selected node to the surface boundary can be generated according to the map; the geodesic distance from the selected node to the surface boundary is the shortest among all the nodes whose Gaussian curvature is higher than a threshold. Using this idea, we can reduce the stretch in the flattened surface by adding shortest cutting paths from high Gaussian curvature nodes to the surface boundary one by one. The cutting paths walk along the triangular edges of the given surface. By generating more cuts from flipped triangles during flattening, even closed surfaces or surfaces with widely distributed curvatures can be cut and flattened.

As a new technique for enhancing the existing surface flattening techniques, our method has the following two advantages compared with other methods based on similar ideas of using cutting paths:

1. our method reaches a faster speed while generating an acceptable result;
2. our method can deal with surfaces with widely distributed curvatures.

Industrial applications of surface flattening impose more requirements on the cutting paths. For example, the direction of the cutting path, or the distribution of the cutting paths may be constrained. Further research can focus on how to incorporate these constraints into the surface flattening technique.

7. References

[1] Carmo M.P.D., *Differential Geometry of Curves and Surfaces*, Prentice Hall, Englewood Cliffs, NJ, U.S.A, 1976.

[2] Kobbelt L.P., Bischoff S., Botsch M., Kähler K., Rössl C., Schneider R., and Vorsatz J., "Geometric modeling based on polygonal meshes", EUROGRAPHICS 2000 Tutorial.

[3] Sheffer A., "Spanning tree seams for reducing parameterization distortion of triangulated surface", SMI 2002: International Conference on Shape Modelling and Applications.

[4] Parida L., Mudur S.P., "Constraint-satisfying planar development of complex surfaces", Computer-Aided Design, vol.25, no.4, pp225-232, 1993.

[5] Aono M., Denti P., Breen D.E., and Wozny M.J., "Fitting a woven cloth model to a curved surface: dart insertion", IEEE Computer Graphics & Applications, vol.16, no.5, pp.60-70., 1996.

[6] Aona M., Breen D.E., and Wozny M.J., "Modeling methods for the design of 3D broadcloth composite parts", Computer-Aided Design, vol.33, no.13, pp.989-1007, 2001.

[7] McCartney J., Hinds B.K., and Seow B.L., "The flattening of triangulated surfaces incorporating darts and gussets", Computer-Aided Design, vol.31, no.4, pp.249-260, 1999.

[8] Kim S.M., Kang T.J., "Garment pattern generation from body scan data", Computer-Aided Design, to appear.

[9] Wang C.C.L., Smith S.S.F., and Yuen M.M.F., "Surface flattening based on energy model", Computer-Aided Design, vol.34, no.11, pp.823-833, 2002.

[10] Cormen T.H., Lieseron C.E., Rivest R.L., *Introduction to Algorithms*, MIT Press, Cambridge, 2000.

[11] Dijkstra E.W., "A note on two problems in connection with graphs", Numerische Mathematik, vol.1, pp.269-271, 1959.

[12] Lanthier M.A., Maheshwari A., and Sack J.-R., "Approximating weighted shortest paths on polyhedral surfaces", Proceedings of 13th ACM Symposium on Computational Geometry, pp.274-283, 1997.

[13] Kanai T., Suzuki H., "Approximate shortest path on a polyhedral surface and its applications", Computer-Aided Design, vol.33, no.11, pp.801-811, 2001.

[14] Thorup M., "Undirected single source shortest paths in linear time", Proceedings of 38th IEEE Symposium on Foundations of Computer Science, pp.12-21, 1997.

[15] Press W.H., *Numerical recipes in C: the art of scientific computing*, Cambridge University Press, 1992.

[16] Gu X., Gortler S.J., Hoppe H., "Geometry Images", SIGGRAPH 2002 Conference Proceedings, 2002.